

Original Research Article

**THERMAL AND FREQUENCY STABILITY OF
DIELECTRIC CERAMIC $\text{Ba}_{6-3x}\text{Nd}_{8+2x}\text{Ti}_{18}\text{O}_{54}$
($x=0.15, 0.25$)**

ABSTRACT

A new dielectric material, barium neodymium titanate (BNT) ceramic can provide good thermal and frequency stability on the dielectric properties. The synthesis of BNT ceramics with $x=0.15$ and 0.25 was carried out using wet solid state method. The ceramics were characterized by X-ray diffraction to identify the phase. The shifting of XRD peaks revealed that higher content of neodymium ions inside the compound. Surface morphology of the ceramics was determined using FESEM. Different compositions influenced the grain growth of the ceramics. BNT ceramics with higher neodymium content showed higher porosity, and higher resistance to shrinkage. The dielectric properties at low frequency from 40 Hz to 1 MHz were measured using Impedance Analyzer. The polarization effect inside the material was discussed and compared. BNT ceramics with $x=0.15$ has higher dielectric constant. These BNT ceramics showed the frequency and thermal stability with respect to the dielectric constant.

Keywords: Dielectric properties; Microstructure; Polarization; Thermal stability

1. INTRODUCTION

The dielectric properties of most dielectric ceramics always show temperature and frequency dependence [1-8]. The change in dielectric constant of a ceramic makes it the difficult to design the materials for use at a certain temperature. Li et al. [9] studied a dielectric material, $\text{BaTiO}_3\text{-Na}_{0.5}\text{Bi}_{0.5}\text{TiO}_3\text{-Nb}_2\text{O}_5\text{-MgO-Glass}$ with Nd_2O_3 addition, and found the capacitance decreases when temperature increases. Su et al. [10] reported the relaxation behaviour of $\text{TbCo}_{0.5}\text{Mn}_{0.5}\text{O}_{3.07}$ ceramics change with increasing temperature. Zaman et al. [11] showed there are two peaks showing temperature dependent of the dielectric constant in the temperature range of 500°C . Adhlakha et al. [12] revealed hopping of Fe ions is thermally activated in $\text{Ni}_{0.75}\text{Zn}_{0.25}\text{Fe}_2\text{O}_4$ doped with BiFeO_3 composites that affect the dielectric constant. Mocanu et al. [13] reported that $\text{Mg}_x\text{Ni}_{1-x}\text{Fe}_2\text{O}_4$ ceramic displays flatten semicircular arc in complex impedance plot that pointed out the electrical properties of that material is frequency dependent. One of the excellent dielectric ceramics is barium titanate, which has a high dielectric constant [14]. However, BaTiO_3 ceramic has a curie temperature around 125°C [15, 16] which point to the changing behaviour of ferroelectric to paraelectric. Araujo [17] studied Curie point in barium calcium titanate solid solution and found Curie temperature increases with increasing calcium ions. At this critical temperature, the dielectric constant starts to reduce and influences the properties of the material. In this research, we have design a dielectric material that has good thermal stability and frequency independent dielectric properties. Addition of neodymium ions into barium titanate resulted in the exchange of phase from perovskite to tungsten bronze structure. It has been reported by Korchagina et al. [18] that neodymium has excellent results in low frequency and microwave

dielectric properties of $\text{Ba}_2\text{LnTaO}_6$ compared to other rare earth elements. Ohsato [19] analysed the structural properties of tungsten bronze type solid solutions by discussing the lattice parameters and positions of the ions inside the compound. Dielectric ceramic with compositional formula $\text{Ba}_{6-3x}\text{Nd}_{8+2x}\text{Ti}_{18}\text{O}_{54}$, BNT ($x=0.15$) was prepared, and the microstructure and dielectric properties were investigated. In order to understand the important role of diffusion of neodymium ions, another dielectric ceramic BNT with $x=0.25$ was also fabricated and material properties were compared.

2. MATERIAL AND METHODS

The raw materials BaCO_3 , Nd_2O_3 , and TiO_2 powders with particle size below 100 nm were used in this work. All powders were mixed and milled using liquid agent ethanol by magnetic stirring method [11]. The powders were weighed according to the desired composition, and milled for 24 hours. After the milling process, the slurries were dried for another 24 hours. The final dried powders were pressed into pellets with diameter of 17 mm and thickness of 2.8 mm. The pellets were then sintered for 3 hours in air in a programmable furnace at 1300°C . BNT with $x=0.15$ and 0.25 were prepared in this work. The density of the samples was measured using Archimedes' principle. The structural properties of the ceramics were determined by X-ray diffractometer (Phillips Expert Pro PW3040) with $\text{CuK}\alpha$ radiation ($\lambda=1.5404\text{\AA}$). The microstructure of the ceramics was observed using FESEM. The dielectric properties of the samples were measured using Impedance Analyzer (Agilent Model 4294A) from 40 Hz to 1 MHz at different measuring temperatures, from room temperature to 250°C .

3. RESULTS AND DISCUSSION

The XRD pattern of BNT ceramics with $x=0.15$ and 0.25 at sintering temperature of 1300°C are shown in Fig. 1. It is found that both samples have a tungsten bronze type with orthorhombic structure [19] without any secondary phases, and the patterns were similar. It is clearly shown as Fig. 1 that both ceramics have many sharp peaks located in the 2θ range, and the highest peak was situated around 31 to 32 degrees. Based on the similar pattern of both ceramics, it is necessary to zoom into the highest peak in order to investigate the relationship of the patterns and the compositions. The comparison of XRD peak between the two compositions of BNT ceramics are given in inset figure of Fig. 1. It can be observed that the highest peak of BNT sample shows shifting to the higher angle when higher Nd ions were doped into the system, which indicates that there are more Nd ions fully incorporated into A1 site of the tungsten bronze type structure which caused distortion in the lattice arrangement. The internal spacing of the arrangement atoms decreases when there is more barium ions replaced by neodymium ions. Interestingly, the shifting behaviour of the peak not only shows the change of the structural distortion, but also could be used to predict the dielectric properties of the sample. The BNT ceramic with $x=0.25$ shows the peak shifted to higher 2θ position meaning that the dielectric constant of this sample would be lower than BNT ceramic with $x=0.15$.

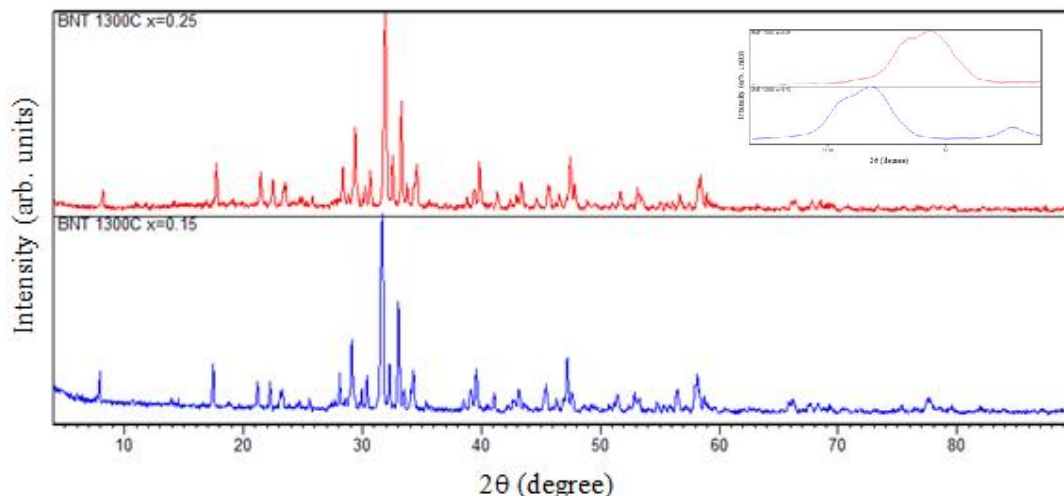


Fig. 1 XRD pattern of BNT ceramic with $x=0.15$ and 0.25 at sintering temperature of 1300°C . Comparison of highest peak of two BNT ceramics (inset figure).

Table 1 shows physical properties of two different compositions of BNT ceramics. It should be mentioned that BNT with $x=0.25$ shows less shrinkage than the other which implies that there is more neodymium atoms present in the sample. It is stated in atomic properties in periodic table [20] that the atomic size of neodymium is bigger than barium atom. Therefore, when there are more barium atoms being replaced by neodymium atoms, the compound has higher resistance to shrinkage. On the other hand, BNT with $x=0.25$ is more porous than BNT with $x=0.15$. It could be related to mass loss during the sintering process. The higher is the mass loss, the smaller is the density. In addition, the increase in porosity might be due to the number of increasing vacancy in the compound. It can be figured out in structural properties of the compound, if the number of barium atoms decrease in A2 site of a tungsten bronze structure [21], then it will create a space. This space could not fill by larger size atoms such as neodymium atom, which made this ceramic becomes less dense.

Table 1. Physical properties of BNT ceramics

Compositions	Density (g cm^{-3})	Shrinkage (%)	Mass loss (%)	Average grain size (μm)
$x=0.15$	4.57	43.59	3.96	0.754
$x=0.25$	3.60	39.73	4.90	0.586

Comparison of surface morphology between different compositions of BNT ceramics is revealed in Fig. 2. The estimated grain size was analysed using linear intercept method by choosing 200 grains inside the sample. The results show that BNT ceramic with $x=0.15$ has bigger grain size than BNT ceramic with $x=0.25$. Both BNT ceramics have fully achieved densification where the grains and grain boundaries can be differentiated clearly on the surface. In view of the grain shape, BNT ceramic with $x=0.25$ did not shows much rectangular grain shape as BNT ceramic with $x=0.15$. Not only that, BNT ceramic with $x=0.25$ displays more porosity on the surface where there is more dark area that was observed in Fig. 3 (b). This porous effect can also be confirmed by the measured density, which reveals the sample has lower density. It could be noticed that, BNT ceramic with more neodymium ions blocked the formation of longer grain shape. The porosity of this sample influenced the dielectric properties of the material. The space between the grains made the

material loses the ability to store charges. This was exhibited in the dielectric results, which shows the higher neodymium content has lower dielectric constant.

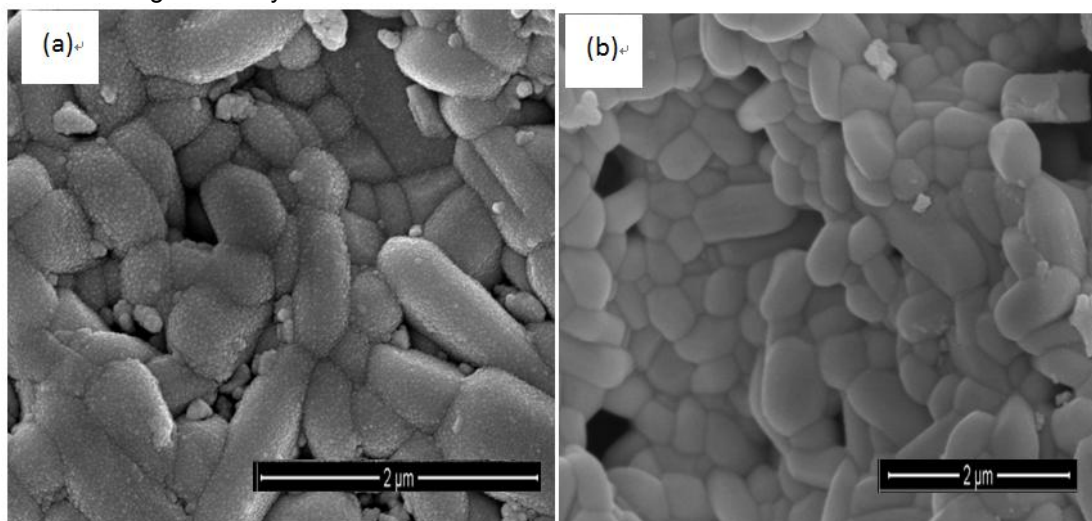


Fig. 2. Microstructure of BNT ceramic sintered at 1300°C; (a) BNT $x=0.15$ and (b) BNT $x=0.25$

Fig. 3 shows the dielectric properties as a function of frequency for BNT ceramics with $x=0.15$ and 0.25 at room temperature and 250°C . The results revealed that the dielectric constant of both ceramics is independent of frequency from 40 Hz to 1 MHz . This property is against the common behaviour of materials which normally showed the dielectric constant decreases with increasing frequency [22-25]. The good frequency stability of these ceramics is normally related to structure of the materials itself. The tungsten bronze type structure always leads the dielectric constant of the material to behave independently of frequency. As can be observed from the results, the Maxwell Wagner type of interfacial polarization [26-28] does not occur in this type of material. In most materials, the dielectric constant is always increased by this polarization effect, especially in the low frequency region. However, the interfacial polarization was eliminated by these two BNT ceramics. This also indicates that there is only orientation polarization [29] occurring in this material. The imaginary part of the dielectric constant or loss factor [30, 31] as a function of frequency for BNT ceramics with $x=0.15$ and 0.25 is shown in Fig. 4. The dielectric loss factor shows a decrease with respect to frequency for both BNT ceramics at all measuring temperatures. No peak can be seen from the results. Therefore, the relaxation of the ceramics could not be defined in this frequency range. The decrement of dielectric loss factor indicates the lossy behaviour of the material can be improved by selecting the correct frequency. On the other hand, when different temperatures were applied to these ceramics, the dielectric loss factor showed no effect at low frequency region. However, loss factor shows a slight increase at high frequency region as temperature increases. This will give an impact to quality factor of the materials. The comparison of dielectric constant as a function of measuring temperature at selected frequency of 1 MHz is given in Fig. 4. The results show that, BNT ceramic with $x=0.15$ has higher dielectric constant. This can be related to several factors. One of the reasons might be related to the shifting behaviour of the highest peak of the ceramics. Besides, the BNT ceramic with $x=0.25$ shows more porosity. On the other hand, both BNT ceramics have good thermal stability in the dielectric constant with the applied measuring temperature. This means that the dipole moment inside the material is already aligned and the poling field did not influenced much on the dipole motions. The dielectric constant showed no much difference indicating these materials can be used in high temperature applications.

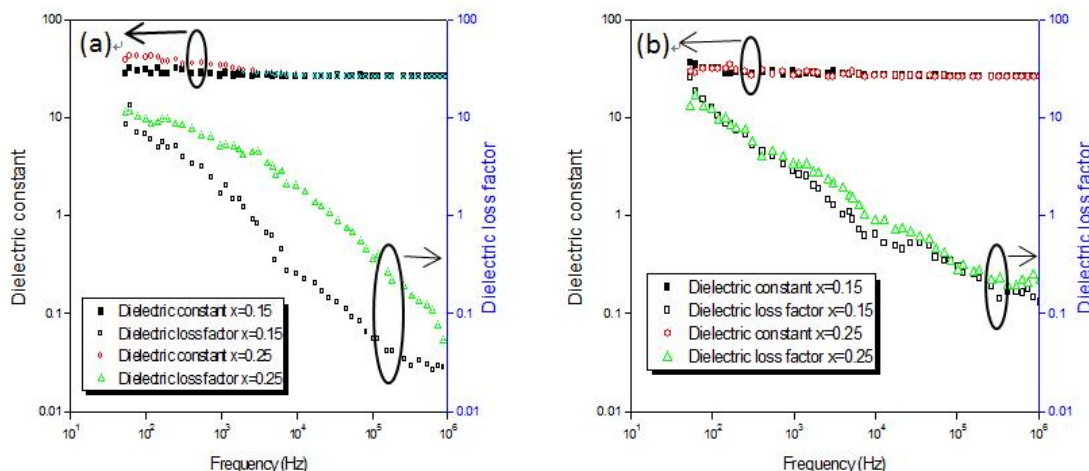


Fig. 3. Dielectric constant and loss factor as a function of frequency: (a) room temperature, (b) 250°C

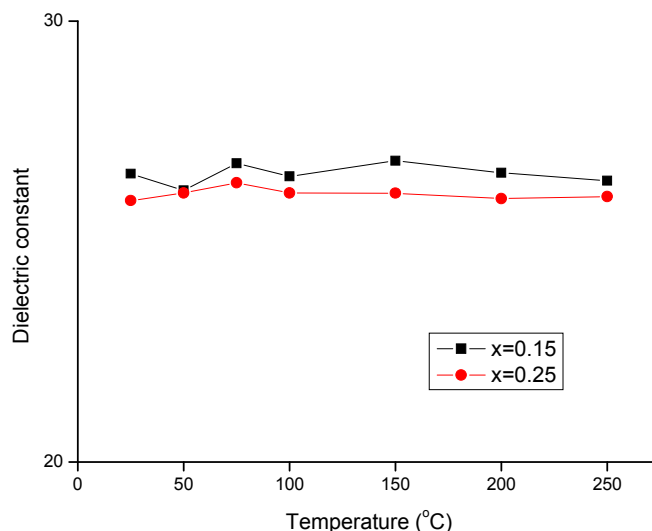


Fig. 4. Dielectric constant as a function of measuring temperature for BNT 0.15 and BNT 0.25 exhibiting thermal stability.

4. CONCLUSION

In conclusion, BNT ceramics with different compositions were fabricated. The shifting of XRD pattern indicates the changing in the interplanar spacing of the compound. BNT ceramic with higher neodymium ions content has higher porosity, and smaller grain size. The dielectric properties show stability in frequency and temperature for both BNT ceramics. Increasing of neodymium ions led to the decrease in the dielectric constant in the tungsten bronze structure. Due to the frequency independence of the dielectric constant, these types of materials can also be used in microwave technology and telecommunication system.

170

171 REFERENCES

172

173 1. Wang JY, Zhang XY, Zhang JJ, Li HL, Li ZF. Dielectric and Piezoelectric Properties
174 of $(1-x)\text{Ba}_{0.7}\text{Sr}_{0.3}\text{TiO}_3-x\text{Ba}_{0.7}\text{Ca}_{0.3}\text{TiO}_3$ Perovskites. Journal of Physics and Chemistry
175 of Solids.2012;73.7:957-960.

176 2. Kumar Patel P, Rani J, Adhlakha N, Singh H, Yadav KL. Enhanced Dielectric
177 Properties of Doped Barium Titanate Ceramics. Journal of Physics and Chemistry of
178 Solids.2013;74.4:545-549.

179 3. Lin D, Huang D, Zhang QJ. Structure, Dielectric and Piezoelectric Properties of
180 $\text{K}_{0.5}\text{Na}_{0.5}\text{NbO}_3-\text{Bi}_{0.5}(\text{Na}_{0.7}\text{K}_{0.2}\text{Li}_{0.1})_{0.5}\text{TiO}_3$ Ceramics. Journal of Physics and
181 Chemistry of Solids. 2013; 74.7: 1021-1025.

182 4. Kar SK and Kumar P. Structural, Morphological and Dielectric Study of
183 $\text{Ba}(\text{FeNb})_{0.5}\text{O}_3$ Ceramics Synthesized by Microwave Processing Technique. Journal of
184 Physics and Chemistry of Solids.2013;74.10:1408-1413.

185 5. Sun ZX, Pu YP, Dong ZJ, Hu Y, Wang PK, Liu XY, Wang Z. Impact of Fast
186 Microwave Sintering on the Grain Growth, Dielectric Relaxation and Piezoelectric Properties
187 on $\text{Ba}_{0.18}\text{Ca}_{0.02}\text{Ti}_{0.09}\text{Zr}_{0.10}\text{O}_3$ Lead-Free Ceramics Prepared by Different Methods.
188 Materials Science and Engineering: B. 2014;185.0:114-1122.

189 6. Madhu BJ, Ashwini ST, Shruthi B, Divyashree BS, Manjunath A, Jayanna HS.
190 Structural, Dielectric and Electromagnetic Shielding Properties of Ni-Cu nanoferrite/PVP
191 Composites. Materials Science and Engineering: B.2014;186.0:1-6.

192 7. Mandal SK, Dey P, Nath TK. Structural, Electrical and Dielectric Properties of
193 $\text{La}_{0.7}\text{Sr}_{0.3}\text{MnO}_3-\text{ErMnO}_3$ Multiferroic Composites. Materials Science and Engineering: B.
194 2014;181.0:70-76.

195 8. Varalaxmi N and Sivakumar KV. "Structural and Dielectric Studies of Magnesium
196 Substituted NiCuZn Ferrites for Microinductor Applications." Materials Science and
197 Engineering: B.2014;184.0:88-97.

198 9. Li LX, Guo D, Xia WS, Liao QW, Han YM, Peng Y. An ultra-broad working
199 temperature dielectric material of BaTiO_3 -based ceramics with Nd_2O_3 addition. Journal of
200 the American Ceramic Society. 2012;95(7):2107-2109.

201 10. Su J, Zhang JT, Lu XM, Lu CJ, He J, Li QC, Zhu JS. Magnetic and Dielectric
202 Properties of Metamagnetic $\text{TbCo}_{0.5}\text{Mn}_{0.5}\text{O}_{3.07}$ Ceramics. Journal of Materials
203 Science.2014;49.10: 3681-3686.

204 11. Zaman A, Iqbal Y, Hussain A, Kim MH, Malik RA. Dielectric, Ferroelectric, and Field-
205 Induced Strain Properties of Ta-doped $0.99\text{Bi}_{0.5}(\text{Na}_{0.82}\text{K}_{0.18})_{0.5}\text{TiO}_3-0.01\text{LiSbO}_3$
206 Ceramics. Journal of Materials Science.2014; 49.8: 3205-3214.

207 12. Adhlakha N, Yadav KL. Structural, Dielectric, Magnetic, and Optical Properties of
208 $\text{Ni}_{0.75}\text{Zn}_{0.25}\text{Fe}_2\text{O}_4-\text{BiFeO}_3$ Composites. Journal of Materials Science.2014;49.13:4423-
209 4438.

- 210 13. Mocanu ZV, Airimioaei M, Ciomaga CE, Curecheriu L, Tudorache F, Tascu S,
211 Iordan AR, Palamaru NM, Mitoseriu L. Investigation of the Functional Properties of
212 $\text{Mg}_x\text{Ni}_{1-x}\text{Fe}_2\text{O}_4$ Ceramics. *Journal of Materials Science* 49.8 (2014): 3276-86.
- 213 14. Ctibor P, Seiner H, Sedlacek J, Pala Z, Vanek P. Phase stabilization in plasma
214 sprayed BaTiO_3 . *Ceramic International*.2013;39(5): 5039–5048
- 215 15. Badheka P, Qi L, Lee B. Phase transition in barium titanate nanocrystals by
216 chemical treatment. *Journal of the European Ceramic Society*.2006; 26(8):1393–1400
- 217 16. Araujo VD, Motta FV, Marques APA, Paskocimas CA, Bomio MRD, Longo E,
218 Varela JA. Effect of Calcium on the Structural Properties of $\text{Ba}_{(1-x)}\text{Ca}_x\text{TiO}_3$ Particles
219 Synthesized by Complex Polymerization Method. *Journal of Materials Science*.2014;49.7:
220 2875-2878.
- 221 17. Korchagina SK, & Shevchuk YA. Low-frequency and microwave dielectric properties
222 of $\text{Ba}_2\text{LnTaO}_6$ (Ln = La, Pr, Sm, Dy, Ce, Gd, Nd, Tm, Tb) ceramics. *Inorganic*
223 *Material*.2006;42(1):64-67.
- 224 18. Ohsato H. Science of Tungstenbronze-Type Like $\text{Ba}_6\text{-}3x\text{R}_8\text{+}2x\text{Ti}_{18}\text{O}_{54}$ (R=rare
225 Earth) Microwave Dielectric Solid Solutions. *Journal of the European Ceramic Society*.2001;
226 21.15: 2703-2711.
- 227 19. Pornprasertsuk R, Yuwapattanawong C, Permkittikul S, Ungtitham T. Preparation
228 of doped BaZrO_3 and BaCeO_3 from nanopowders. *International Journal of Precision*
229 *Engineering and Manufacturing*.2012;13(10):1813-1819.
- 230 20. David R. Lide, ed., *CRC Handbook of Chemistry and Physics*, 90th Edition (CD-
231 ROM Version 2010), CRC Press, Taylor and Francis, Boca Raton, FL
- 232 21. Chen YC and Huang CL. Microwave dielectric properties of $\text{Ba}_2\text{-}x\text{Sm}_4\text{+}2/3x\text{Ti}_9\text{O}_{26}$
233 ceramics with zero temperature coefficient. *Materials Science and Engineering A334* (2002)
234 250–256.
- 235 22. Yan M, Tan YQ, Zhao H, Peng J, Xiao XL, Hu ZB. Crystal Structure, Dielectric and
236 Magnetic Properties of $\text{Ba}_5\text{NdNi}_{1.5}\text{Nb}_{8.5}\text{O}_{30}$ Tungsten Bronze Ceramic. *Materials*
237 *Chemistry and Physics*.2012;136.2: 487-491.
- 238 23. Fang, L, Xiang F, Liao W, Liu LJ, Zhang H, Kuang XJ. Dielectric Properties and
239 High-Temperature Dielectric Relaxation of $\text{Ba}_3\text{Ti}_4\text{Nb}_4\text{O}_{21}$ Ceramic. *Materials Chemistry*
240 *and Physics*.2014;143.2: 552-556.
- 241 24. Chen J W, Narsinga Rao G, Lee HM, Lee WL, Chou FC. Dielectric Properties of the
242 Spin-1/2 Dimer Compounds $\text{Ba}_3\text{Cr}_2\text{O}_8$ and $\text{Sr}_3\text{Cr}_2\text{O}_8$. *Materials Chemistry and*
243 *Physics*.2014;145.3: 461-464.
- 244 25. Cao WQ. and Chen W. Dielectric Properties of Y_2O_3 Donor-Doped $\text{Ba}_{0.8}\text{Sr}_{0.2}\text{TiO}_3$
245 Ceramics. *Materials Chemistry and Physics*.2014;143.2: 676-680.
- 246 26. Samkaria R, Sharma V. Effect of Rare Earth Yttrium Substitution on the Structural,
247 Dielectric and Electrical Properties of Nanosized Nickel Aluminate. *Materials Science and*
248 *Engineering: B*.2013;178.20: 1410-1415.

- 249 27. Maxwell JC. A Treatise on Electricity and Magnetism, vol. 2, Dover Publications:
250 Oxford, NY; 1954.
- 251 28. Koops CG. Phys. Rev. 83.1951; 121–124.
- 252 29. Raju GG. Polarization and static dielectric constant. Dielectrics in Electric Fields.
253 CRC Press: 2003
- 254 30. Raju GG. Dielectric loss and relaxation - I. Dielectrics in Electric Fields. CRC Press:
255 2003.
- 256 31. Raju GG. Dielectric loss and relaxation - II. Dielectrics in Electric Fields. CRC Press:
257 2003.